



# A complementary approach to estimate the internal pressure of fission gas bubbles by SEM-SIMS-EPMA in irradiated nuclear fuels

C. Cagna, I. Zacharie-Aubrun, P. Bienvenu, L. Barrallier, B. Michel, J. Noirot

## ► To cite this version:

C. Cagna, I. Zacharie-Aubrun, P. Bienvenu, L. Barrallier, B. Michel, et al.. A complementary approach to estimate the internal pressure of fission gas bubbles by SEM-SIMS-EPMA in irradiated nuclear fuels. IOP Conference Series: Materials Science and Engineering, IOP Publishing, 2016, 109, pp.012002. 10.1088/1757-899X/109/1/012002 . cea-02432835

HAL Id: cea-02432835

<https://hal-cea.archives-ouvertes.fr/cea-02432835>

Submitted on 8 Jan 2020

**HAL** is a multi-disciplinary open access archive for the deposit and dissemination of scientific research documents, whether they are published or not. The documents may come from teaching and research institutions in France or abroad, or from public or private research centers.

L'archive ouverte pluridisciplinaire **HAL**, est destinée au dépôt et à la diffusion de documents scientifiques de niveau recherche, publiés ou non, émanant des établissements d'enseignement et de recherche français ou étrangers, des laboratoires publics ou privés.

PAPER • OPEN ACCESS

## A complementary approach to estimate the internal pressure of fission gas bubbles by SEM-SIMS-EPMA in irradiated nuclear fuels

To cite this article: C Cagna *et al* 2016 *IOP Conf. Ser.: Mater. Sci. Eng.* **109** 012002

View the [article online](#) for updates and enhancements.

### Related content

- [Determination of xenon concentrations in nuclear fuels by electron microprobe analysis](#)

C Ronchi and C T Walker

- [Development of Xe and Kr empirical potentials for CeO<sub>2</sub>, ThO<sub>2</sub>, UO<sub>2</sub> and PuO<sub>2</sub>, combining DFT with high temperature MD](#)

M W D Cooper, N Kuganathan, P A Burr *et al.*

- [Kinetics of fission gas release](#)

K Forsberg and A R Massih

### Recent citations

- [Changing the rules of the game: used fuel studies outside of a remote handling facility](#)

Jon M. Schwantes *et al*

- [Theoretical study of xenon adsorption on UO<sub>2</sub> surfaces](#)

Jack Arayro *et al*

# A complementary approach to estimate the internal pressure of fission gas bubbles by SEM-SIMS-EPMA in irradiated nuclear fuels

**C Cagna<sup>1</sup>, I Zacharie-Aubrun<sup>1</sup>, P Bienvenu<sup>1</sup>, L Barrallier<sup>2</sup>, B Michel<sup>1</sup> and J Noirot<sup>1</sup>**

<sup>1</sup> CEA Cadarache, DEN, DEC, 13108 Saint-Paul-lez-Durance, France

<sup>2</sup> Arts et Métiers ParisTech, Laboratory MSMP, 2 Cours des Arts et Métiers, 13617 Aix-en-Provence, France

E-mail: celine.cagna@cea.fr

**Abstract.** The behaviour of gases produced by fission is of great importance for nuclear fuel in operation. Within this context, a decade ago, a general method for the characterisation of the fission gas including gas bubbles in an irradiated UO<sub>2</sub> nuclear fuel was developed and applied to determine the bubbles internal pressure. The method consists in the determination of the pressure, over a large population of bubbles, using three techniques: SEM, EPMA and SIMS. In this paper, a complementary approach using the information given by the same techniques is performed on an isolated bubble under the surface and is aiming for a better accuracy compared to the more general measurement of gas content. SEM and EPMA enable the detection of a bubble filled with xenon under the surface. SIMS enables the detection of the gas filling the bubble. The quantification is achieved using the EPMA data as reference at positions where no or nearly no bubbles are detected.

## 1. Introduction

The behaviour of rare gases produced by fission is of great importance for nuclear fuel in operation. It controls the release in the free volume and hence the internal pressure of the fuel rod, the fuel swelling and also part of the behaviour of the fuel during off-normal situations or accidental events. During the operation of a Pressurized Water Reactor (PWR), the fuel is subjected to different loads - mainly mechanical and thermal - that modify its behaviour when combined with the effects of irradiation. The irradiation generates fission gases (Xe and Kr) in the fuel pellets, which are generally found in bubble form, from nanometre to micrometre diameters. Fission gases behaviour in oxides fuels has been the focus of attention for decades because of their impact on the overall behaviour of the fuel rod. During accidents such as RIA (Reactivity Initiated Accident) or LOCA (Loss of Coolant Accident), increasing temperature in the pellets leads to grain boundary fracturing, release of intergranular gases and rod over-pressurisation. The internal pressure of the bubbles can be high and thus generate internal stress in the fuel. Evaluating this pressure is a key matter especially for nuclear safety aspects.

A method has been developed in CEA to improve the description of the fission gas behaviour [1-3]. This method consists in a collection of complementary experimental results. These measurements are supporting the fission gas model MARGARET [4].

It has been shown that the characterisation of irradiated samples with SIMS (secondary ion mass spectrometry) is possible, and that xenon can be measured on irradiated UO<sub>2</sub> fuel [1-3]. Xenon filling



Content from this work may be used under the terms of the [Creative Commons Attribution 3.0 licence](#). Any further distribution of this work must maintain attribution to the author(s) and the title of the work, journal citation and DOI.

the bubbles is detected as peaks measured during a depth profile [3-5]. It has been demonstrated that the total xenon inventory can be quantitatively measured from a large number of detected peaks and the pressure inside the bubbles deduced [6, 7]. The statistical analysis of the gas quantity inside bubbles can be compared to the statistical characterisation of porosity obtained with SEM (scanning electron microscopy) in order to get a mean atomic volume of xenon inside the bubbles.

In this paper, a complementary methodology is proposed to evaluate the internal pressure of xenon in fission gas bubbles in an irradiated nuclear fuel pellet using three microanalysis techniques: SEM/SIMS/EPMA (electron probe microanalyser). In order to get more refined results and a comprehensive gas inventory of the nuclear fuel, it is no longer based on statistical method from many bubbles but on a single bubble analysis. This work was initiated [8] but the main difficulty was to isolate one bubble.

This breakthrough in the description of fission gas inventory will enrich the data base used for code validation and is expected to lead to significant improvement in the understanding of fission gas behaviour.

## 2. Experimental

### 2.1. Sample

The sample used for this study was a large grain UO<sub>2</sub>, with an initial <sup>235</sup>U enrichment of 4.89 %. It was taken from a French PWR fuel rod with zircaloy cladding, irradiated for 2 cycles and ramped at 470 W.cm<sup>-1</sup> during 12 h. The local burn-up at the sampling position was calculated to be 38.8 GWd/t<sub>M</sub>. The sample was embedded in a metallic alloy with a low melting point to ensure good electrical conductivity and polished to get a plane surface.

### 2.2. Equipment

The same sample was examined by shielded SEM, EPMA and SIMS for radioactive material characterisation.

SEM was performed with a shielded XL 30 model (PHILIPS) with a Centaurus KE developments BSE (backscattered electron) and SE (secondary electron) detectors and a SIS (Soft Imaging Solutions) ADDA image acquisition device to obtain 4096 x 4096 pixels images covering large areas with high definition.

EPMA was performed with a shielded CAMEBAX model (CAMECA). Xenon was analysed using the Lα-line of the characteristic X-ray with a PET crystal. Xenon radial distribution and mapping were measured at an electron acceleration potential of 30 kV and an incident beam current of 250 nA. The acquisition time was 20 s. Quantitative analysis of xenon was carried out using an UO<sub>2</sub> (irradiated at low temperature to 25 GWd/t<sub>U</sub>) standard, multi-characterized [9].

SIMS was performed with a shielded IMS 6f (CAMECA). The <sup>132</sup>Xe depth profile was measured with a 20 nA oxygen primary beam focussed on a 40 μm diameter area. <sup>132</sup>Xe signal was measured during 0.2 s periods. On irradiated samples, the xenon signal measured with SIMS must be separated from the molecular interferences produced by fission products, especially from <sup>100</sup>Mo<sup>16</sup>O<sub>2</sub><sup>+</sup>. The interferences were avoided thanks to an energy filter (offset + 50 V): the ions energy depends on the location at which the atoms or molecules are ionized. The xenon ions are created over the sample surface while most of the other ions are created at the surface, allowing us to neglect the local environment effect on the measurement of the gas out of the bubble.

### 2.3. Procedure

**2.3.1. Selection of the region of interest.** The first step was to localize an area where bubbles were large and where the bubble density was low enough to isolate a single bubble under the surface. A global view of the sample surface and an image of the pellet radius are shown in figure 1. In this paper, the positions of the examination points are given relatively to the radius of the pellet: 1R is the periphery of the pellet, 0R is its centre.

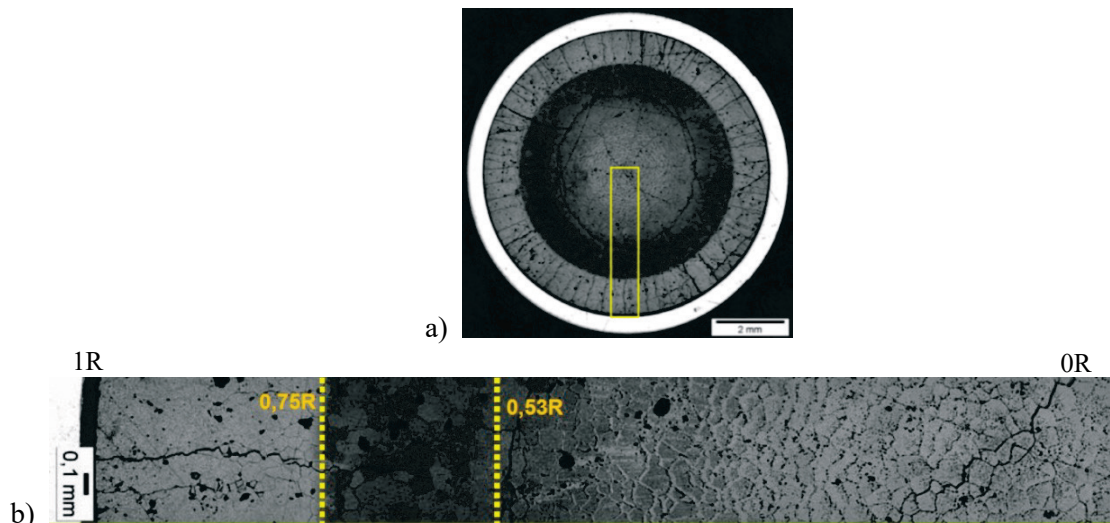


**Figure 1.** Macrograph of the polished cross-section sample (a) and detail along a radius (b).

The global methodology [4] for the determination of the bubbles internal pressure was carried out on this sample. Xenon was measured with SIMS by making depth profiles regularly spaced along the same radius that was analysed by EPMA. The xenon signal was measured as a function of time while a 80  $\mu\text{m}$  diameter area was sputtered with a 60 nA  $\text{O}_2^+$  primary current during 5,000 s (figure 1).

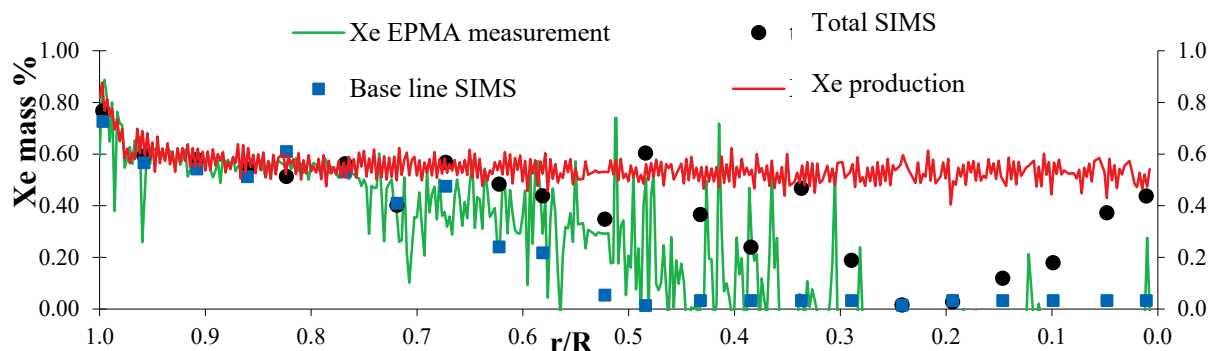


**Figure 2.** Comparison between the EPMA xenon measurement and the SIMS baseline ( $R$ : pellet radius,  $r$ : radial position).

The three techniques, SEM, EPMA and SIMS provide a consistent and complementary description of the gas inventory. Between 0.8R and 0.9R, in the bulk of the grains, xenon is either dissolved or precipitated in too small bubbles to be evidenced with SIMS or EPMA; a relative lack of xenon around the grain boundaries and scarce bubbles are observed. At the centre, the total xenon concentration is lower than the production.

In the central area, mean pressure was deduced from the global methodology and estimated at 9.1 MPa and bubble diameters were around 1.2  $\mu\text{m}$ .

To implement the new approach on a single bubble, the centre is a suitable area (see figure 3). The large grain size is interesting for our studies in particular compared to the beam diameter of the SIMS that is around 40 - 50  $\mu\text{m}$ . Figure 3b shows grain boundaries with lenticular bubbles (green) and

grains with spherical intragranular bubbles (red) with an average equivalent diameter between 1 and 2  $\mu\text{m}$ . Their density ( $108 \text{ mm}^{-3}$ ) is well suited to allow counting a small number of bubbles. The area selected for the study, figure 3b, is situated inside a grain and consequently only concerns intragranular bubbles.

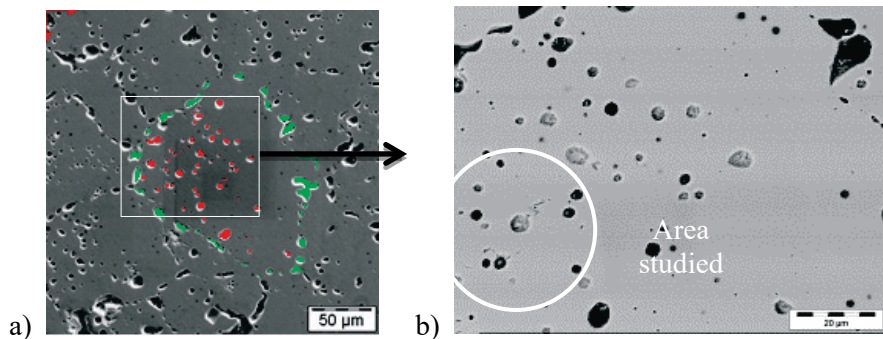


**Figure 3.** SEM images of a) the central zone, and b) grain selected for the study (BSE - 25 kV).

**2.3.2. Localisation of bubbles under the surface.** The localisation of bubbles just under the surface was carried out by both SEM and EPMA observations. Figures 4a and 4b present SEM images and xenon X-ray maps obtained with EPMA on a small part of the working area before and after ion sputtering with SIMS. With SEM, the investigation was performed by working with two detectors (SE and BSE) and at different electron acceleration voltages, from 10 to 30 kV. This method is discussed in the next section. In the following paragraphs, SEM images were obtained at 25 kV. In figure 4a, the green circles point out the presence of a bubble uncut by polishing and still filled with fission gases. BSE images show the presence of a cavity (green circle). Not detected by the SE image, this cavity is below the polished plane. The EPMA X-ray map of Xe shows that this cavity, though close to the surface, is still filled with Xe (bright spot).

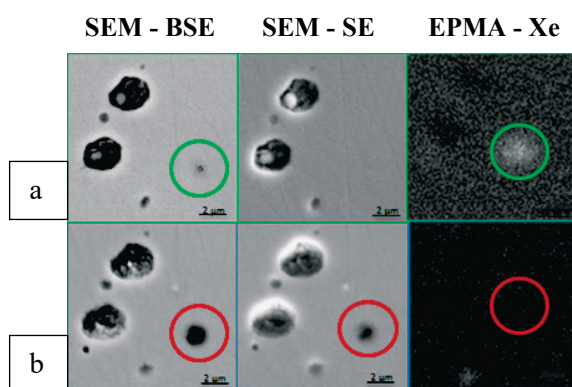


**Figure 4.** SEM SE, BSE images and EPMA X cartographies showing the evolution of one bubble before (a) and after (b) SIMS abrasion (enlarged images on a bubble).

**2.3.3. Abrasion with SIMS.** When a bubble is selected, a first depth profile with SIMS is performed. The diameter of the ion beam is controlled by the voltage and the current. The diameter of the spot, obtained with 15 kV and 20 nA, was around 50  $\mu\text{m}$ . The acquisition was stopped when a peak with a

high intensity was observed (hypothesis, one peak = one bubble). At this stage, we assumed that one bubble has been opened and that the new surface after sputtering was situated in the first half of the bubble above its median plan. Work is ongoing in order to improve the measurement of the bubble diameter (see section 4.2).

**2.3.4. Control of bubble opening.** The peak obtained with SIMS needs to be associated with a bubble. In order to check if it does correspond to the bubble selected previously, the sample was observed a second time with EPMA. Figure 4b, shows the same area as figure 4a, but after the short sputtering period. On BSE and SE images, most of the bubbles appear unchanged. However, the initially uncut bubble is now appearing more clearly on the BSE image, and is detectable with the SE image. With the X-ray map, the release of Xe from the bubble appears clearly.

**2.3.5. Evaluation of bubble diameter.** The determination of the bubble diameter was performed after SIMS abrasion. The sample was placed a second time in the SEM and it was measured by image analysis taking into account the black halo around the bubble considered as the maximum diameter. The accuracy of this method is discussed in the next section.

**2.3.6. Synoptic of the overall methodology.** Figure 5 is a schematic view of the single bubble methodology.

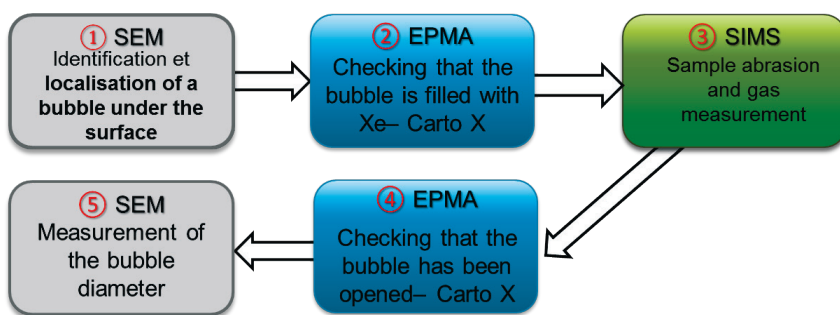


**Figure 5.** Procedure for the single bubble methodology using SEM, EPMA and SIMS.

### 3. Results

The procedure has been applied on the UO<sub>2</sub> sample and the results are described and explained up to the calculation of the bubble pressure.

#### 3.1. SIMS results

Figure 6 presents the xenon signal measured with SIMS as a function of the sputtering time. The measurement has been performed with <sup>132</sup>Xe isotope. As soon as one large peak is observed, the acquisition is stopped because it is considered that the number of peak is related to the number of bubbles observed by SEM. Two components are seen:

- a baseline which is associated to <sup>132</sup>Xe solid solution or nanobubbles,
- 3 significant peaks coming from the bubbles.

Between 15 and 120 seconds, an average baseline can be determined. It is then subtracted from the whole profile. The intensity of the highest peak is assumed to be associated to xenon that was contained in the largest opened bubble.

#### 3.2. Quantification of the xenon inventory

A quantitative evaluation of xenon concentration is possible using the experimental results obtained with SIMS and EPMA [1]. At the centre, the EPMA measurement shows almost no xenon in solution

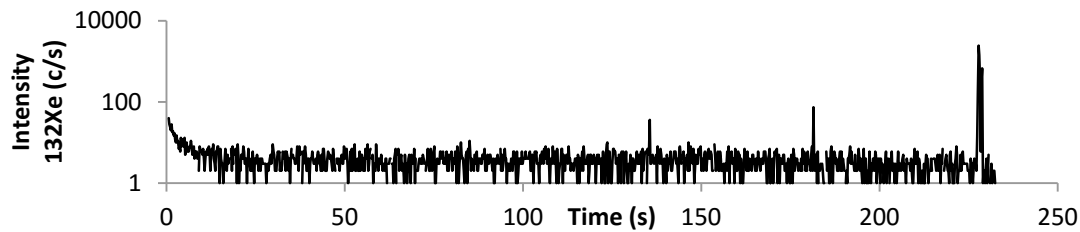


**Figure 6.** SIMS depth profile of Xe-132.

(figure 2). However, at the mid-radius position, the xenon is considered to be totally in solid solution because no bubble was detected by SIMS or observed by SEM. At this position, both EPMA and SIMS measurements are equal to the quantity produced during the irradiation and can be directly compared and correlated. For a given material, the sputtering yield depends on the microstructure (including grain crystalline orientation) and the impurities it contains. The sputtered surface is not large enough to average the effect of the crystalline orientation of the UO<sub>2</sub> grains but several SIMS acquisitions at the same position (mid-radius) and a work on the average data helps reducing the effect of grain orientation. Besides, the compositions and burn-up of the mid-radius and centre areas are relatively close. For example, figure 2 showing the radial Xe production profile deduced from Nd, exhibits no major change from the mid-radius to the centre. Thus the composition should not have a significant effect on the sputtering yield.

The mean volume of the SIMS craters is calculated and with the abrasion time, we can deduce a sputtering speed and a volume per count. The mass of UO<sub>2</sub> corresponding to this volume is obtained and thanks to the xenon concentration measured from EPMA, it is possible to calculate the quantity of xenon corresponding to one count.

The quantity of xenon n<sub>Xe</sub> (mol) is obtained through the following relation (1):

$$n_{Xe} = I_{(c/s)} f \quad (1)$$

with the factor  $f = \frac{W_{\%Xe} V_c \rho_{UO_2}}{I_m M_{Xe}}$  and  $I_{(c/s)}$  the intensity of the peak corresponding to one bubble,

where:  $W_{\%Xe}$ : weight % of xenon (EPMA results),  $V_c$ : mean crater volume ( $m^{-3}$ ),  $\rho_{UO_2}$ : UO<sub>2</sub> density ( $g.m^{-3}$ ),  $M_{Xe}$ : molar mass of xenon ( $g.mol^{-1}$ ), and  $I_m$ : mean intensity in the mid-radius position ( $c.s^{-1}$ ).

### 3.3. SEM results

SEM observations are useful to localize bubbles under the surface prior to SIMS analysis. Then, it allowed us to determine the diameter,  $d$ , and thus the volume,  $V$ , of the bubbles opened by SIMS with the hypothesis that the bubbles are spherical. The SEM images of the other bubbles, cut during the polishing process show that this hypothesis is reasonable for intragranular bubbles, even if a perfect sphericity is not observed (figure 4).

### 3.4. Pressure results

From the SIMS results and the bubble volume measured, it is then possible to obtain a molar volume of xenon for the bubble with the relation (2):

$$V_m = \frac{V}{n_{Xe}} \quad (2)$$

Xenon is not the only atom present in its gas form at room temperature [10]. Indeed, krypton has to be considered in the calculation of the pressure. A ratio is used between Xe and Kr obtained from neutronic calculations assuming the same behaviour for both gases. In order to calculate the bubble pressure, an equation of state is needed. Several equations can be found in the literature and behave differently depending on the domain of temperature and molar volume. Some experimental data are available for Xe. For example, Ronchi [11] has extrapolated confidently the high temperature and high density pressure–volume–temperature data of Xe using a Leonard–Jones (LJ) interatomic potential.

Comparisons have been carried out between those experimental results and equations of state.

The Soave equation (3) [12] is in good agreement with the experimental data for a molar volume larger than  $40 \text{ cm}^{-3} \cdot \text{mol}^{-1}$  which is the case of the measurements here. With the application of mixing rules, the equation can be extended to multicomponent calculations (Xe + Kr).

$$P_g = \frac{RT}{(V_m - b_M)} - \frac{a_M}{(V_m^2 + cb_M V_m + db_M^2)} \quad (3)$$

Mixing rules:  $a_M = (\sum x_i a_i^{0.5})^2$ ,  $b_M = \sum x_i b_i$  and  $x_i$  fraction of the element  $i$  (depending on the ratio xenon/krypton calculated).

With:

$$a_i = \frac{a_0 R^2 T_c^2}{P_c} \text{ and } a_0 = 0.42748(1 + f(1 - (\frac{T}{T_c})^{1/2}))^2$$

$$b_i = b_0 R \frac{T_c}{P_c}, b_0 = 0.0866; c = 1; d = 0;$$

For xenon: critical temperature,  $T_c = 289.70 \text{ K}$ ; critical pressure,  $P_c = 5.84 \times 10^6 \text{ Pa}$  and  $f = 0.492$ .

For krypton: critical temperature,  $T_c = 209.35 \text{ K}$ ; critical pressure,  $P_c = 5.50 \times 10^6 \text{ Pa}$  and  $f = 0.488$ .

The methodology has been applied on several bubbles. Table 1 gives their diameter, molar volume and pressures at room temperature calculated with (3).

**Table 1.** Pressure results for several bubbles.

	Bubble diameter (nm) ( $\pm 200$ )	Molar volume ( $\text{cm}^3 \cdot \text{mol}^{-1}$ )	Pressure at 300 K (MPa)
<b>1</b>	300	59.1	32.8
<b>2</b>	1,600	52.52	56.4
<b>3</b>	400	68.3	19.3
<b>4</b>	2,100	182	7.1
<b>5</b>	2,100	178	7.1
<b>6</b>	400	177	7.1
<b>7</b>	600	440	4.3
<b>8</b>	1,900	10,397	0.2
<b>9</b>	1,900	641	3.2

## 4. Discussion

### 4.1. Comparison with experimental results

The results can be compared with other experimental data obtained with different techniques on irradiated fuels. Nogita and Une [13] determined the Xe density in nanometric bubbles with EDS. Noirot [6] and Walker [7] used SIMS to measure the Xe quantity. Noirot's and Walker's values correspond to the high burn-up structure (HBS) from UO<sub>2</sub> and MOX fuels at the periphery and mid-radius for the first author and from a UO<sub>2</sub> fuel at the periphery for the second. All these published data therefore correspond to situations very far from the sample studied here.

The results obtained with the method presented in this paper are represented figure 7 and data from the literature are also reported. The graph gives a schematic correlation between bubble internal pressure and bubble radius for irradiated UO<sub>2</sub> fuels, in which the equilibrium pressure ( $P_{eq} = 2\gamma/r$ ;  $\gamma$ : surface energy;  $r$ : bubble radius) is given. The pressures were calculated at room temperature (300 K).

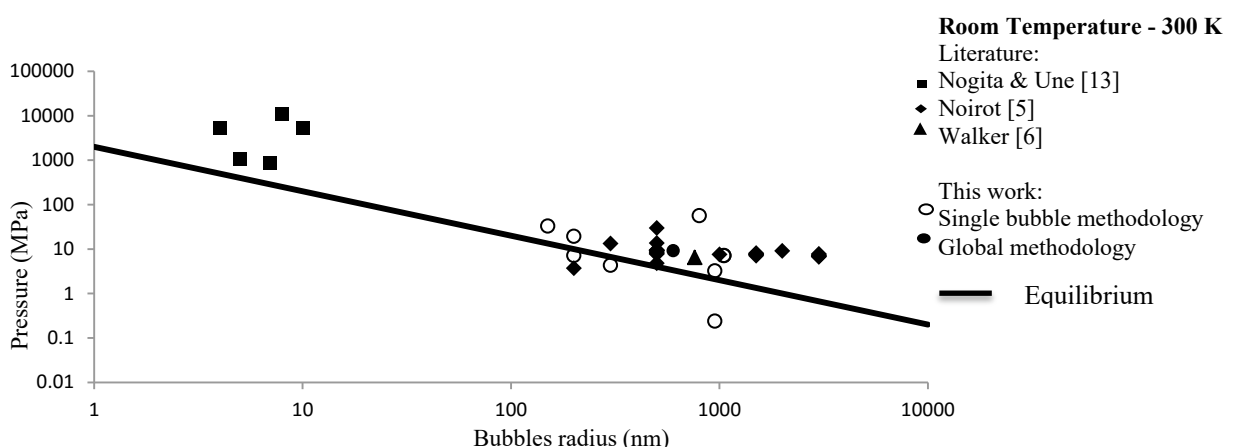


**Figure 7.** Experimental data of fission gas bubbles, pressure of xenon versus their radius.

The single bubble approach and the global methodology were all applied on the same sample. The mean pressure is close to the equilibrium (3 MPa) at room temperature. This means that in spite of the ramp and high temperatures, it was, like HBS bubbles at the periphery or nanobubbles, clearly over-pressurized in pile. The individualized bubble pressures are also around this equilibrium, at room temperature, but highly scattered, with pressures above equilibrium and pressures under equilibrium. Those results cannot be directly compared to the values from the literature. The areas studied are different but they globally seem to be in the same order of magnitude (around 10 MPa) and they tend to be over-pressurized or close to the equilibrium except for one value.

Besides, the pressure results do not conform to the evolution of the equilibrium law and figure 7 shows a large variation of the pressures from 50 MPa to less than 10 MPa. Indeed, the pressures are not inversely proportional to the radius. For a diameter of 400 nm (see table 1), the equilibrium pressure is 10 MPa and a bubble contains gas at a pressure of 22.9 MPa (over-pressurized), whereas the other shows its pressure decrease at 6 MPa (slightly under-pressurized). Without more work on the uncertainty, it is difficult to conclude if this observation is a result of a real variation in the nuclear fuel or if it is a consequence of the uncertainty of the method.

#### 4.2. Accuracy

The errors introduced in the pressure calculation come from the measurement of the quantity of xenon and the measure of the bubble diameter.

The accuracy of the xenon concentration obtained with this procedure is a function of the EPMA xenon concentration accuracy and of SIMS experimental parameters which are difficult to measure. Their evaluation is investigated by performing tests on the different sources of uncertainty such as the sample and standard, instruments, effects of experimental conditions (current, counting rate, background noise, ...) and data post-treatment.

The second source of error is of great importance. The diameter is obtained by the analysis of 2D images involving 3D effects and is raised to the cube in the calculation of the volume. Some hypotheses are taken into account and work is ongoing in order to validate or improve them.

With the single bubble approach, it is complicated to determine if the surface is situated just at the median plan of the bubble. Several measurements have been carried out with SEM images obtained with different high tensions, before and after SIMS abrasion. It seems that the bubbles open at their top with a burst of gas, the pressure being too strong. In the case of micrometric bubbles just opened after a SIMS abrasion, BSE detector at high tensions enables to perceive the bubbles diameter close to its maximum (figure 8).

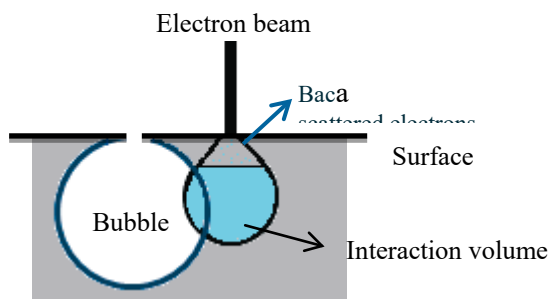


**Figure 8.** Localisation of the new surface after a SIMS abrasion - electron interactions.

The uncertainty associated with the determination of the diameter is estimated at  $\pm 200$  nm for micrometric bubbles. A new SEM replacing the device used for this study, with higher capacities and especially a FIB (focussed ion beam), will be used to better characterise the bubbles and reduce this major uncertainty.

Besides, during the first SIMS abrasion, 3 bubbles were opened (figure 6). For the post-treatment of the SIMS depth profiles, we assumed that one bubble corresponds to one pic and that the highest pic is associated to the largest bubble. This is tested by changing the order of attribution in order to identify aberrations (such as a pressure of 1 GPa in a bubble from the centre of the nuclear fuel).

The sources of error are identified and work is carried out in order to evaluate the total uncertainty.

#### 4.3. Detection of bubbles under the surface

The detection of bubbles with SEM is the first step that enables us to get easily a view of the bubbles located under the surface. Figure 9 presents SEM images of the same area that were carried out with both detectors, BSE and SE and at different tensions, from 10 to 30 kV.

It appears that a bubble close enough to the surface becomes visible by increasing the tension and with a better contrast using BSE detector sensitive to electrons that come from deeper. For image analysis, in order to obtain the bubble size distribution from opened bubbles, it is then recommended to work at low voltage (10 kV). On the contrary, high voltage (25 - 30 kV) is necessary in order to visualize with good contrast bubbles that are around 0.25 to 0.5  $\mu\text{m}$  deep in  $\text{UO}_2$  samples (Monte Carlo simulation).

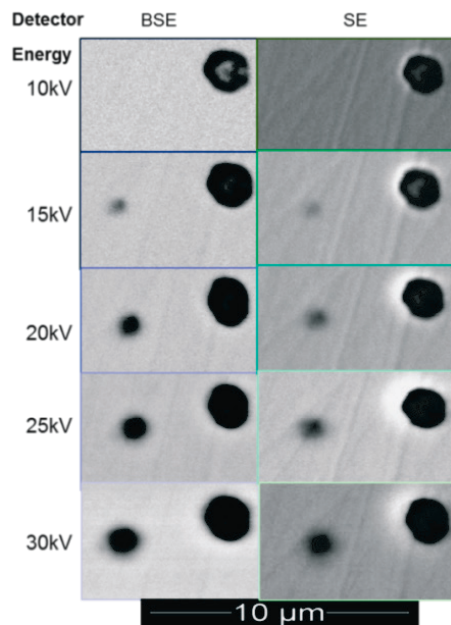


**Figure 9.** Appearance of a bubble detected with SEM using BSE and SE detectors at electron acceleration voltages from 10 to 30 kV.

## 5. Conclusion

We have described a new approach that combines three techniques in a high activity laboratory that enable the determination of individual fission gas bubble pressure in irradiated fuels. The method has been developed to get more refined results on a few bubbles, for the best case, one. It is complementary to the global methodology established a decade ago. The method has been applied to the central part of a ramped UO<sub>2</sub> irradiated fuel. This paper has shown that:

- The quantity of xenon coming from a single bubble can be measured, quantified and used to determine the pressure.
- In order to get closer to the case of a single bubble, some improvement will be made especially for the ion beam diameter. A compromise is needed between the diameter and the intensity of the beam (xenon ionisation rate).

The uncertainty coming from the measurement of the bubble diameter has been estimated, but the total uncertainty needs to be completely investigated. It will be improved with a FIB-SEM available soon in the laboratory, in order to get a 3D view of the microstructure. Several sources of errors were highlighted and work is carried out in order to obtain the total uncertainty.

## Acknowledgments

The authors are indebted to Electricité de France and Areva for their support.

## References

- [1] Desgranges L and Pasquet B 2004 *Nucl. Instr. Meth. B* **215** 545-551
- [2] Noirot J, Noirot L, Desgranges L, Lamontagne J, Blay T, Pasquet B and Muller E 2004 *Proc. of the International topical meeting on LWR fuel performance*. (Orlando, FL, USA) **1019** 329
- [3] Lamontagne J, Desgranges L, Valot C, Noirot J, Blay T, Roure I and Pasquet B 2006 *Microchim. Acta* **87** 183-187
- [4] Noirot L 2011 *Nucl. Engng. Des.* **241** 2099-2118
- [5] Desgranges L, Valot C, Pasquet B, Lamontagne J, Blay T and Roure I 2008 *Nucl. Instr. Meth. B* **266** 147-154
- [6] Noirot J, Desgranges L and Lamontagne J 2008 *J. Nucl. Mater.* **372** 318-339

- [7] Walker C T, Bremier S, Portier S, Hasnaoui R and Goll W 2009 *J. Nucl. Mater.* **393** 212-223
- [8] Lamontagne J, Noirot J, Desgranges L, Blay T, Pasquet B and Roure I 2004 *Microchim. Acta* **145** 91-94
- [9] Boidron M, Tourasse M, Boussard F, Piron J P and Pasquet B 1991 *Proc. of the International topical meeting on LWR fuel performance*. (Avignon, France) 21-24
- [10] Valin S 1999 PhD-thesis (Grenoble, France: INP)
- [11] Ronchi C 1981 *J. Nucl. Mater.* **96** 314-328
- [12] Soave G 1972 *Chem. Engng. Sci.* **27** 1197-1203
- [13] Nogita K and Une K 1998 *Nucl. Instr. Meth. B* **11** 481-486